

Range Resolution of Near-field MIMO Sensing

Marcin Wachowiak, *Member, IEEE*, André Bourdoux, *Senior Member, IEEE*, Sofie Pollin, *Member, IEEE*,

Abstract—The radiative near-field and integration of sensing capabilities are seen as two key components of the next generation of wireless communication systems. In this paper, the sensing performance of a narrowband near-field system is investigated for several practical antenna array geometries and configurations, namely SIMO/MISO and MIMO. In the SIMO/MISO configuration, the antenna aperture is exploited only a single time for either transmit or receive signal processing, while the MIMO configuration exploits both TX and RX processing. Analytical derivations, supported by simulations, show that the MIMO processing improves the maximum near-field range and sensing resolution by approximately a factor of 1.4 as compared to single-aperture systems. The value of the improvement factor is consistent for all considered array geometries. Finally, using a quadratic approximation of the array factor, an analytical improvement factor of $\sqrt{2}$ is derived, clarifying the observed improvements and validating the numerical results.

Index Terms—Radiative near-field, finite-depth beamforming, near-field beamforming, near-field sensing, MIMO

I. INTRODUCTION

A. Problem Statement

The radiative near-field (NF) systems are regarded as a key enabler of the next generation of wireless systems [1]. Their ability to create beamspots in the distance domain enables user multiplexing both in range and angle [2], [3]. This unique property has also attracted the attention of the sensing community as beamfocusing in the range domain can be utilized to localize the targets with limited bandwidth [4], [5]. Despite these advantages, near-field sensing performance is subject to significant shortcomings, such as limited resolution, maximum near-field range and poor peak-to-sidelobe level (PSL) performance. The recent research regarding near-field sensing has largely focused on single-array geometry and single-aperture systems [3]–[7]. To improve the near-field sensing, the performance gains from MIMO sensing have to be identified and quantified for different array geometries.

B. Relevant works

In [6], the near-field beam focusing was derived for a uniform square array, based on electromagnetic principles. Generalizations of the array factor (AF) in the near-field for arbitrary uniform rectangular array (URA) and uniform planar circular array (UPCA) are provided in [3]. This work studies the beamfocusing property from a communication-centric perspective. The near-field communications performance and AF of a uniform circular array (UCA) were discussed in [7].

Marcin Wachowiak and Sofie Pollin are with Interuniversitair Micro Electronica Centrum, 3001 Leuven, Belgium and also with the Katholieke Universiteit Leuven, 3000 Leuven, Belgium (e-mail: marcin.wachowiak@imec.be)

André Bourdoux is with Interuniversitair Micro-Electronica Centrum, 3001 Leuven, Belgium. (Corresponding author: *Marcin Wachowiak*)

In [4] the near-field sensing resolution was demonstrated using a testbed equipped with a uniform linear antenna array (ULA). An approximation of the near-field range resolution for the same array architecture and SIMO/MISO case is provided in [5]. The sensing performance of a near-field system for point and extended targets was investigated in [8]. This work discusses the NF performance of the SIMO/MISO and MIMO systems regarding the Cramér–Rao lower bound, but does not directly discuss the gains from MIMO for point targets.

C. Contributions

In this work, the NF sensing performance is evaluated for several array geometries: ULA, UCA, URA and UPCA. The sensing performance is studied for two cases SIMO/MISO - single aperture and MIMO - two identical exactly collocated apertures. The gains from employing MIMO are assessed in terms of resolution, maximum NF range and PSL level of the ambiguity function. Based on a quadratic approximation, the analytical improvement factor is derived, which matches well with the numerical simulations.

II. SIGNAL MODEL

A. Ambiguity function of near-field sensing system

Consider a collocated narrowband antenna array with M transmitters and N receivers. The location of the m th transmitter is given by \mathbf{p}_m and n th receiver by \mathbf{p}_n . The antenna elements are assumed to be isotropic and mutual coupling is considered negligible. The distance between each antenna element and some point in space is $d_m(\mathbf{p}) = \|\mathbf{p} - \mathbf{p}_m\|_2$ for transmitters and $d_n(\mathbf{p}) = \|\mathbf{p} - \mathbf{p}_n\|_2$ for receivers. The bistatic distance is denoted as $d_{m,n}(\mathbf{p}) = d_m(\mathbf{p}) + d_n(\mathbf{p})$. The region of interest is located within the radiative near-field of the array and the propagation is modeled as line-of-sight. The channel can be written as

$$h_{m,n}(\mathbf{p}) = e^{-j2\pi \frac{f}{c} d_{m,n}(\mathbf{p})}. \quad (1)$$

Given the channel model and array configuration, the matched filter response (MF) or ambiguity function for a single frequency and a target at position \mathbf{p}' is

$$\mathcal{A}(\mathbf{p}', \mathbf{p}) = \frac{1}{\sqrt{MN}} \sum_{m \in M} \sum_{n \in N} h_{m,n}(\mathbf{p}') h_{m,n}^*(\mathbf{p}). \quad (2)$$

Note that the formulated ambiguity function does not consider bandwidth and is valid only for a single frequency. The ambiguity function can be separated into the product of two sums as follows

$$\begin{aligned} \mathcal{A}(\mathbf{p}', \mathbf{p}) &= \frac{1}{\sqrt{M}} \sum_{m \in M} e^{-j2\pi \frac{f}{c} \Delta d_m(\mathbf{p}', \mathbf{p})} \\ &\times \frac{1}{\sqrt{N}} \sum_{n \in N} e^{-j2\pi \frac{f}{c} \Delta d_n(\mathbf{p}', \mathbf{p})}. \end{aligned} \quad (3)$$

where $\Delta d_m(\mathbf{p}', \mathbf{p}) = d_m(\mathbf{p}') - d_m(\mathbf{p})$ and $\Delta d_n(\mathbf{p}', \mathbf{p}) = d_n(\mathbf{p}') - d_n(\mathbf{p})$ is the distance difference between \mathbf{p}' and \mathbf{p} for m th and n th antenna. The per antenna distance difference can be expressed as a distance difference with regard to the reference antenna element ($m = 0$ and $n = 0$) and a distance difference dependent on the antenna index

$$\Delta d_m(\mathbf{p}', \mathbf{p}) = \Delta d_{m=0}(\mathbf{p}', \mathbf{p}) + \delta d_m(\mathbf{p}', \mathbf{p}) \quad (4)$$

$$\Delta d_n(\mathbf{p}', \mathbf{p}) = \Delta d_{n=0}(\mathbf{p}', \mathbf{p}) + \delta d_n(\mathbf{p}', \mathbf{p}). \quad (5)$$

This allows to express the matched filter in terms of array factors as

$$\begin{aligned} \mathcal{A}(\mathbf{p}', \mathbf{p}) = & e^{-j2\pi\frac{c}{f}\Delta d_{m=0}(\mathbf{p}', \mathbf{p})} \underbrace{\frac{1}{\sqrt{M}} \sum_{m \in M} e^{-j2\pi\frac{f}{c}\delta d_m(\mathbf{p}', \mathbf{p})}}_{\text{AF}_{\text{TX}}(\mathbf{p}', \mathbf{p})} \\ & \times e^{-j2\pi\frac{c}{f}\Delta d_{n=0}(\mathbf{p}', \mathbf{p})} \underbrace{\frac{1}{\sqrt{N}} \sum_{n \in N} e^{-j2\pi\frac{f}{c}\delta d_n(\mathbf{p}', \mathbf{p})}}_{\text{AF}_{\text{RX}}(\mathbf{p}', \mathbf{p})}. \quad (6) \end{aligned}$$

To calculate the power of the MF, the phase offsets can be removed, leading to

$$|\mathcal{A}(\mathbf{p}', \mathbf{p})|^2 = |\text{AF}_{\text{TX}}(\mathbf{p}', \mathbf{p})|^2 |\text{AF}_{\text{RX}}(\mathbf{p}', \mathbf{p})|^2. \quad (7)$$

The MIMO configuration improves the ambiguity function by introducing a multiplication by a second array factor compared to SIMO/MISO case, where only a single array factor defines the ambiguity function. In the near-field region, the AF depends both on angle and distance from the array, unlike in the far-field, where it is only angle dependent. The distance sensitivity results in an array gain that varies with distance and facilitates the beamfocusing. The distance dependence of the AF leverages new applications allowing to discriminate targets and users located at the same angle but different distances without the use of bandwidth, which is not possible in the far-field.

B. Near-field 3 dB beamdepth

Consider a target and points of interest located along the array normal, this allows to reduce the vectors \mathbf{p} , and \mathbf{p}' to scalars d and d' , which represent the distance from the weight center of the array along the normal. The AF in the near-field can be calculated analytically for different array architectures. [3], [6], [7]. Due to the Fresnel approximation of distance in the NF of the array, the argument of the AF shares the same formula for different array architectures

$$x(d, d') = ad_{\text{FA}}d_{\text{ver}} \quad (8)$$

where a is a scalar dependent on the array geometry, $d_{\text{FA}} = 2D^2/\lambda$ is the Fraunhofer distance of the array, D is the array aperture, λ is the wavelength and $d_{\text{ver}} = |\frac{1}{d} - \frac{1}{d'}| = \frac{|d'-d|}{dd'}$ is the absolute value of vergence difference [9]. For brevity in the following, the shorthand x is used to represent $x(d, d')$. Consider some near-field ambiguity function given by $|\mathcal{A}(x)|^2$. For a SISO/SIMO system, the ambiguity function will be defined by a single array factor of the transmit or receive aperture $|\mathcal{A}(x)|_{\text{SISO/MISO}}^2 = |\text{AF}(x)|^2$. For the MIMO scheme, the

ambiguity function will be a product of two array factors. For simplicity, the transmit and receive arrays are considered to be identical and exactly collocated, resulting in a monostatic system $|\mathcal{A}(x)|_{\text{MIMO}}^2 = |\text{AF}(x)|^4$.

The range resolution is evaluated in terms of the radial half-power beamwidth of the ambiguity function, also referred to as the beamdepth (BD). The 3 dB beamdepth is calculated by computing the argument for which the ambiguity function reaches half of the maximum value. Considering normalized ambiguity function it can be written as $|\mathcal{A}(x_{3\text{dB}})|^2 = 0.5$. The argument value is then used to calculate the distance d at which the -3 dB value is reached by solving (8) for d resulting in

$$d_{3\text{dB}} = \frac{d_{\text{FA}}d'}{d_{\text{FA}} \pm \alpha d'}. \quad (9)$$

Formula (9) gives two distances for which the -3 dB value is achieved for target at d' , where $\alpha = x_{3\text{dB}}/a$. The parameter a depends only on the array geometry, while $x_{3\text{dB}}$ depends on both the array architecture and configuration SIMO/MISO or MIMO. As $d_{3\text{dB}}$ should always be positive, the following constraint arises $d' < \frac{d_{\text{FA}}}{\alpha}$. Given the -3 dB crossing points, 3 dB beamdepth (BD) is

$$BD = \begin{cases} \frac{2\alpha d_{\text{FA}}d'^2}{d_{\text{FA}}^2 - \alpha^2 d'^2}, & d' < \frac{d_{\text{FA}}}{\alpha}, \\ \infty, & d' \geq \frac{d_{\text{FA}}}{\alpha}. \end{cases} \quad (10)$$

For d greater or equal to $\frac{d_{\text{FA}}}{\alpha}$ the beamdepth extends from d_{FA}/α to infinity. Note that parameter α determines both the 3 dB beamdepth resolution and the maximum near-field distance for which the BD is finite. In the following sections, the α parameter is computed for different array architectures to assess the resolution and maximum near-field sensing range.

III. RESULTS

A. Uniform Linear Array (ULA)

Consider a uniform linear array with element spacing lower than or equal to $\lambda/2$. For points at the broadside of the array, the NF AF can be approximated as [3]

$$\begin{aligned} |\text{AF}_{\text{ULA}}(d', d)|^2 = & \quad (11) \\ = & M \frac{4}{d_{\text{FA}}d_{\text{ver}}} \left(C^2 \left(\sqrt{\frac{d_{\text{FA}}d_{\text{ver}}}{4}} \right) + S^2 \left(\sqrt{\frac{d_{\text{FA}}d_{\text{ver}}}{4}} \right) \right), \end{aligned}$$

where $C(u) = \int_0^u \cos(\pi t^2/2) dt$ and $S(u) = \int_0^u \sin(\pi t^2/2) dt$ are Fresnel integrals. For ULA the combined argument of the AF is $x = \frac{d_{\text{FA}}d_{\text{ver}}}{4}$ and hence $a = 1/4$.

1) *SIMO/MISO*: The normalized AF is

$$|\text{AF}(x)|^2 = \frac{C^2(\sqrt{x}) + S^2(\sqrt{x})}{x}. \quad (12)$$

The -3 dB value is achieved for argument $x_{3\text{dB}} = 1.738$, which results in $\alpha = 6.952$.

2) *MIMO*: The normalized AF is

$$|\text{AF}(x)|^4 = \left(\frac{C^2(\sqrt{x}) + S^2(\sqrt{x})}{x} \right)^2. \quad (13)$$

The -3 dB value is achieved for argument $x_{3\text{dB}} = 1.242$, which results in $\alpha = 4.968$.

B. Uniform Circular Array (UCA)

Consider a uniform circular array with antenna elements distributed on a circle of diameter D . Given that the spacing between the antennas is lower than or equal to $\lambda/2$, the NF AF can be approximated as [7]

$$|\text{AF}_{\text{UCA}}(d', d)|^2 = M \left(J_0 \left(\frac{\pi d_{\text{FA}} d_{\text{ver}}}{16} \right) \right)^2, \quad (14)$$

where J_0 denotes the zero-order Bessel function of the first kind. For UCA the combined argument of the AF is $x = \frac{\pi d_{\text{FA}} d_{\text{ver}}}{16}$ and hence $a = \pi/16$.

1) *SIMO/MISO*: The normalized AF is

$$|\text{AF}(x)|^2 = (J_0(x))^2. \quad (15)$$

The -3 dB value is achieved for argument $x_{3\text{dB}} = 1.126$, which results in $\alpha = 5.735$.

2) *MIMO*: The normalized AF is

$$|\text{AF}(x)|^4 = (J_0(x))^4. \quad (16)$$

The -3 dB value is achieved for argument $x_{3\text{dB}} = 0.815$, resulting in $\alpha = 4.151$.

C. Uniform Rectangular Array (URA)

Consider a uniform rectangular array with equal planar dimensions, resulting in a square array. In a square array, the total aperture is measured as the diagonal and equals D . For antenna spacing lower than or equal to $\lambda/2$ and points on the array normal, the NF AF can be approximated as [3]

$$|\text{AF}_{\text{URA}}(d', d)|^2 = M \left(\frac{8}{d_{\text{FA}} d_{\text{ver}}} \right)^2 \left(C^2 \left(\sqrt{\frac{d_{\text{FA}} d_{\text{ver}}}{8}} \right) + S^2 \left(\sqrt{\frac{d_{\text{FA}} d_{\text{ver}}}{8}} \right) \right)^2 \quad (17)$$

For square URA the combined argument of the AF is $x = \frac{d_{\text{FA}} d_{\text{ver}}}{8}$ and hence $a = 1/8$.

1) *SIMO/MISO*: The normalized AF is

$$|\text{AF}(x)|^2 = \left(\frac{C^2(\sqrt{x}) + S^2(\sqrt{x})}{x} \right)^2. \quad (18)$$

The -3 dB value is achieved for argument $x_{3\text{dB}} = 1.242$, which results in $\alpha = 9.936$.

2) *MIMO*: The normalized AF is

$$|\text{AF}(x)|^4 = \left(\frac{C^2(\sqrt{x}) + S^2(\sqrt{x})}{x} \right)^4. \quad (19)$$

The -3 dB value is achieved for argument $x_{3\text{dB}} = 0.884$, which results in $\alpha = 7.072$.

D. Uniform Planar Circular Array (UPCA)

Consider an array implemented as a uniform planar circular array constructed from concentric circles. Given that the spacing between the antenna elements does not exceed $\lambda/2$, the NF AF can be approximated as [3]

$$|\text{AF}_{\text{UPCA}}(d', d)|^2 = M \text{sinc}^2 \left(\frac{d_{\text{FA}} d_{\text{ver}}}{16} \right), \quad (20)$$

where $\text{sinc}(x) = \sin(\pi x)/(\pi x)$. For UPCA the combined argument of the AF is $x = \frac{d_{\text{FA}} d_{\text{ver}}}{16}$ and hence $a = 1/16$.

1) *SIMO/MISO*: The normalized AF is

$$|\text{AF}(x)|^2 = \text{sinc}^2(x). \quad (21)$$

The -3 dB value is achieved for argument $x_{3\text{dB}} = 0.443$, which results in $\alpha = 7.088$.

2) *MIMO*: The normalized AF is

$$|\text{AF}(x)|^4 = \text{sinc}^4(x). \quad (22)$$

The -3 dB value is achieved for argument $x_{3\text{dB}} = 0.319$, which results in $\alpha = 5.104$.

TABLE I
VALUE OF α PARAMETER PER ARRAY GEOMETRY AND PROCESSING.

Array geometry	$\alpha_{\text{SIMO/MISO}}$	α_{MIMO}	Ratio $\frac{\alpha_{\text{SIMO/MISO}}}{\alpha_{\text{MIMO}}}$
ULA	6.952	4.968	1.399
UCA	5.735	4.151	1.382
URA	9.936	7.072	1.405
UPCA	7.088	5.104	1.389

Table I presents the summarized values of the parameter α for each considered array geometry and processing. By comparing the α values across antenna geometries and processing a few observations can be made. The MIMO processing improves the α parameter approximately by the same factor of 1.4 regardless of the array geometry. This corresponds to 1.4-fold improvement in the NF sensing resolution and maximum NF range.

The consistent ratio $\frac{\alpha_{\text{SIMO/MISO}}}{\alpha_{\text{MIMO}}}$ observed across various array geometries can be attributed to quadratic decay of AF within the mainlobe. Based on this, the mainlobe can be accurately approximated as a quadratic function [10]. Since the considered normalized AF is even, with a maximum value of 1, for SIMO/MISO configuration it can be approximated as

$$|\text{AF}(x)|^2 \approx 1 - cx^2, \quad (23)$$

where c is some scalar that controls the decay rate and depends on the array geometry. The -3 dB value is obtained for argument $x_{3\text{dB}}^{\text{SIMO/MISO}} = \frac{\sqrt{2}}{2\sqrt{c}}$.

Next, in the MIMO case, the approximation from (23) is squared. To keep the approximation quadratic for both scenarios, higher order terms are neglected, resulting in

$$|\text{AF}(x)|^4 \approx 1 - 2cx^2. \quad (24)$$

The -3 dB value is obtained for argument $x_{3\text{dB}}^{\text{MIMO}} = \frac{1}{2\sqrt{c}}$. Based on the quadratic approximation the ratio between the SIMO/MISO and MIMO arguments is

$$\frac{x_{3\text{dB}}^{\text{SIMO/MISO}}}{x_{3\text{dB}}^{\text{MIMO}}} = \sqrt{2}. \quad (25)$$

According to the quadratic approximation, introducing the MIMO scheme should reduce the $x_{3\text{dB}}$ argument by a factor $\sqrt{2}$, which corresponds to $\frac{\alpha_{\text{SIMO/MISO}}}{\alpha_{\text{MIMO}}}$ equal to $\sqrt{2}$. Notice that the parameter c , which controls the rate of the decay of the AF mainlobe, does not affect the ratio of the arguments. This confirms the observation from Table I that, although the rate of decay varies across array geometries, the improvement

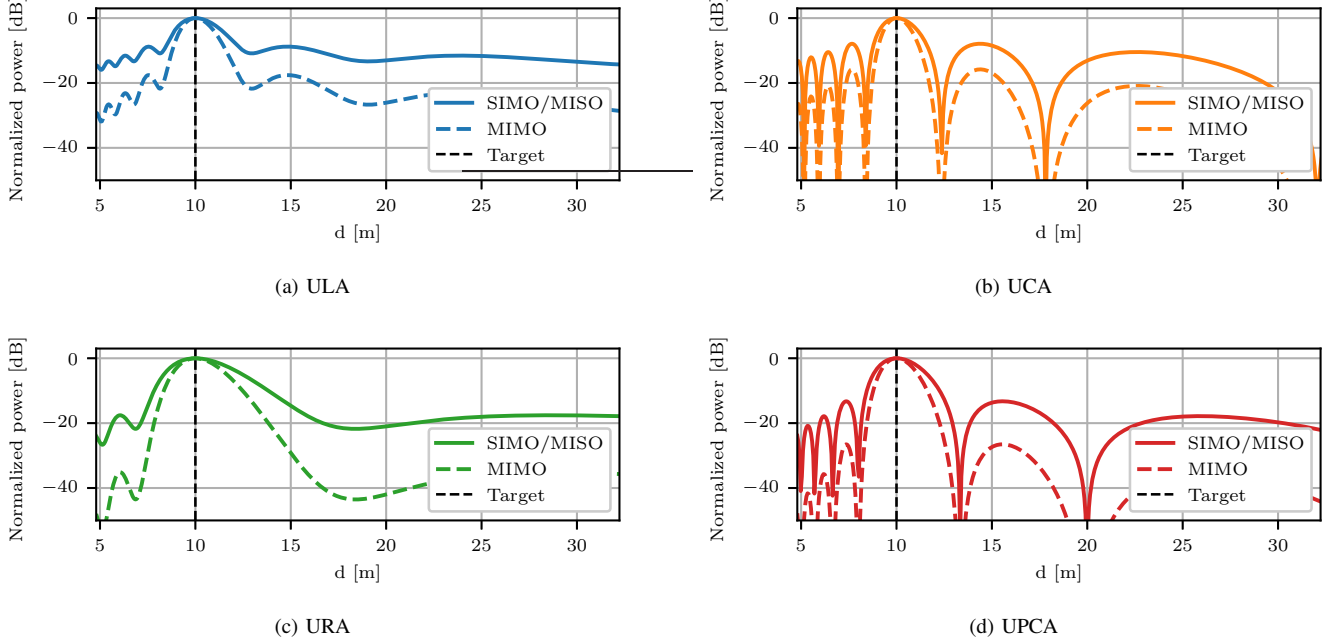


Fig. 1. Ambiguity function for selected antenna arrays and processing. The array aperture is 4m with a center frequency of 6 GHz, the target is located at 10m from the array.

in the argument offered by MIMO is identical. The worst-case relative error introduced by the approximation is below 2.33%, matching well with the numerical results. Fig. 1 illustrates the ambiguity function for each considered array geometry and processing. As anticipated, MIMO processing improves the resolution by offering an array factor that decays at a faster rate. Note that the nulls of the ambiguity function remain the same regardless of the processing, as squaring any arbitrary real function preserves the locations of the zeros.

Moreover, the MIMO processing significantly improves the peak-to-sidelobe level. Squaring of the AF corresponds to multiplication of the decay rate by 2, resulting in a twofold improvement of the PSL, as can be seen in Fig. 1. Table II presents the PSL per antenna geometry and processing. Interestingly, the arrays distributed on a plane (URA, UPCA) offer much better PSL than the one-dimensional arrays (ULA, UCA), although the latter offer better resolution.

TABLE II
PEAK-TO-SIDELOBE LEVEL PER ARRAY GEOMETRY AND PROCESSING.

Array geometry	PSL _{SIMO/MISO} [dB]	PSL _{MIMO} [dB]
ULA	-8.78	-17.57
UCA	-7.9	-17.8
URA	-17.57	-35.14
UPCA	-13.26	-26.52

IV. CONCLUSION

This paper presents and quantifies the gains offered by MIMO configuration in the NF sensing. Independent of the antenna array geometry, MIMO offers an approximate $\sqrt{2}$ improvement in both NF sensing resolution and maximum NF

range as compared to SIMO/MISO scenario. Furthermore, due to squaring of the AF, MIMO processing achieves a twofold improvement of the PSL in the NF.

REFERENCES

- [1] Z. Wang, J. Zhang, H. Du, D. Niyato, S. Cui, B. Ai, M. Debbah, K. B. Letaief, and H. V. Poor, "A tutorial on extremely large-scale MIMO for 6G: Fundamentals, signal processing, and applications," *IEEE Communications Surveys & Tutorials*, vol. 26, no. 3, pp. 1560–1605, 2024.
- [2] H. Zhang, N. Shlezinger, F. Guidi, D. Dardari, M. F. Imani, and Y. C. Eldar, "Beam focusing for near-field multiuser MIMO communications," *IEEE Transactions on Wireless Communications*, vol. 21, no. 9, pp. 7476–7490, 2022.
- [3] A. Kosasih and E. Björnson, "Finite beam depth analysis for large arrays," *IEEE Transactions on Wireless Communications*, vol. 23, no. 8, pp. 10 015–10 029, 2024.
- [4] A. Sakhnini, S. De Bast, M. Guenach, A. Bourdoux, H. Sahli, and S. Pollin, "Near-field coherent radar sensing using a massive MIMO communication testbed," *IEEE Transactions on Wireless Communications*, vol. 21, no. 8, pp. 6256–6270, 2022.
- [5] A. Sakhnini, M. Wachowiak, A. Bourdoux, and S. Pollin, "An approximation of the range resolution in the near-field of a distributed antenna array," *IEEE Wireless Communications Letters*, vol. 13, no. 12, pp. 3281–3284, 2024.
- [6] E. Björnson, Ö. T. Demir, and L. Sanguinetti, "A primer on near-field beamforming for arrays and reconfigurable intelligent surfaces," in *2021 55th Asilomar Conference on Signals, Systems, and Computers*, 2021, pp. 105–112.
- [7] Z. Wu, M. Cui, and L. Dai, "Enabling more users to benefit from near-field communications: From linear to circular array," *IEEE Transactions on Wireless Communications*, vol. 23, no. 4, pp. 3735–3748, 2024.
- [8] G. Thiran, F. De Saint Moulin, C. Oestges, and L. Vandendorpe, "Performance bounds for near-field multi-antenna range estimation of extended targets," in *2024 IEEE 25th International Workshop on Signal Processing Advances in Wireless Communications (SPAWC)*, 2024, pp. 261–265.
- [9] M. Katz, R. Hayes, and G. Zikos, *Introduction to Geometrical Optics*. Penumbra Publishing Company, 1994.
- [10] A. Sakhnini, A. Albaba, A. Bourdoux, and S. Pollin, "A general technique for radar resolution analysis based on a quadratic approximation," *IEEE Transactions on Radar Systems*, vol. 2, pp. 251–262, 2024.